

SENSIVITY STUDIES FOR NUCLEAR ISLAND FOUNDED ON PILES INCLUDING EFFECTS OF SEISMIC MOTION SPATIAL VARIATION AND LOCAL NONLINEAR SOIL BEHAVIOR

Dan M. Ghiocel

Chief of Engineering, Ghiocel Predictive Technologies, Inc., NY, USA (dan.ghiocel@ghiocel-tech.com)

ABSTRACT

The paper investigates the SSI effects for a nuclear complex founded on piles. Both floating piles and peak-bearing piles are considered. The paper investigates the effects of the local nonlinear soil behaviour in the vicinity of piles. The effects of inclined S-P incident waves are also included. The paper presents various SSI result comparisons including nuclear complex ISRS, structural displacements, and pile forces and moments. Comparisons between SSI results for the “without piles” and the “with piles” cases are included. The seismic SSI analysis is performed using the ACS SASSI software (Ghiocel, 2019) that can simulate incoherent motion random wavefields via an accurate Monte Carlo method implementation and include the local soil nonlinear hysteretic behaviour using an efficient iterative equivalent-linearization numerical procedure. The paper offers an useful practical guidance for SSI modelling of the pile foundations within the SASSI flexible volume substructuring approach. The SASSI model captures accurately both the kinematic and inertial SSI effects that are both important for an accurate prediction of the pile foundation SSI behaviour. In addition, the local soil nonlinear hysteretic behaviour in the vicinity of piles is included.

DESCRIPTION OF THE INVESTIGATED PROBLEMS

The paper investigates the seismic SSI effects for a nuclear complex founded on concrete piles, as shown in Figure 1. The nuclear complex foundation area is about 250 ft x 300 ft. The nuclear RB complex has its basemat at the grade level, basically sitting on the pile foundation.

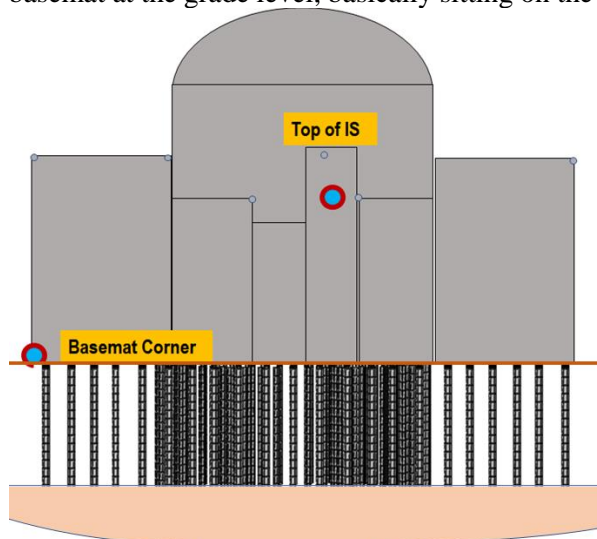


Figure 1. Nuclear Complex on Pile Foundation

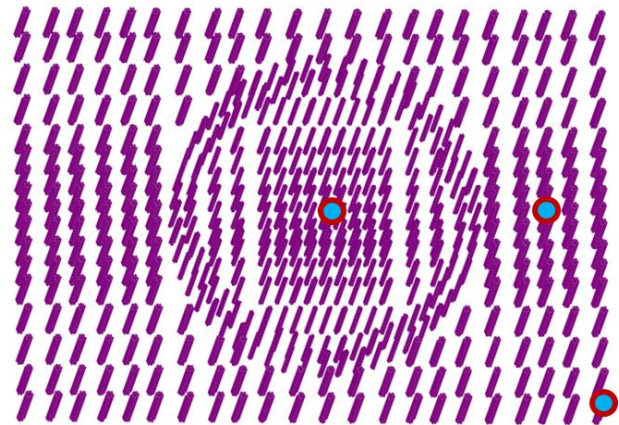


Figure 2. Pile Locations Under Basemat

The pile foundation depth is 60 ft below the grade level. Figure 2 shows the locations of the 495 concrete piles under the basemat. The concrete piles have either 3 ft or 4.5 ft diameter. The highest density of the concrete piles is under the reactor containment building (RB) as shown in Figure 2. The piles surrounding the RB have larger spacings.

The soil deposit is modelled for two situations as shown in Figure 3: 1) Case A: Uniform deep soft soil deposit with V_s varying between 750 fps 900 fps, and 2) Case B: Soft soil layer of 60 ft thickness with V_s varying between 750 fps and 900 fps sitting above a rock formation with V_s of 5,500 fps.

The seismic input motions for the horizontal and vertical directions are defined by the spectrum-compatible acceleration motions generated based on the outcrop ground response spectra (GRS) at the at the pile foundation level at the 60 ft depth. The outcrop GRS correspond to the European type GRS for medium soil sites as shown in Figure 4 for one horizontal direction (target GRS with black line, and computed GRS with red line). The in-column GRS computed at the pile foundation level is shown also in Figure 4 (with blue line).

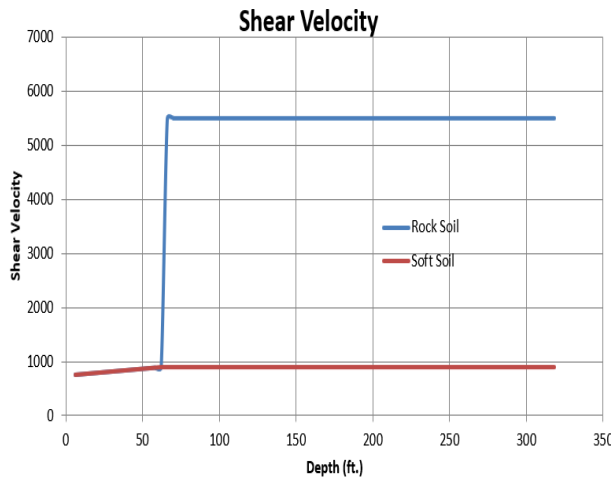


Figure 3. The Two V_s Soil Profiles Considered

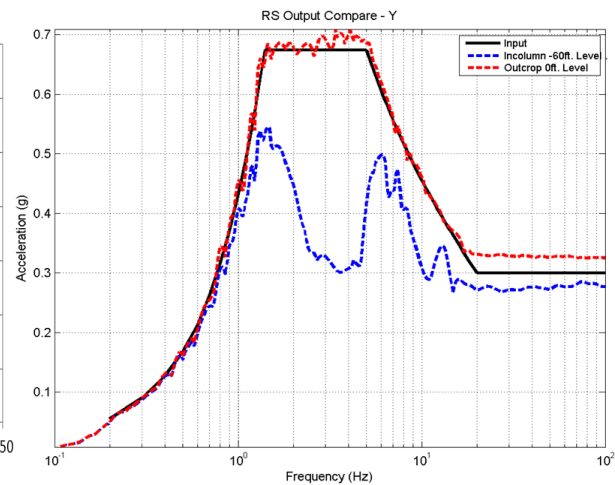


Figure 4. The GRS at the Pile Foundation Depth

For the incoherent SSI analysis, the rigorous stochastic simulation approach (with no phase adjustment) was used. A number of 20 incoherent simulated wavefields were used to compute the (mean) incoherent SSI responses. The incoherency model was defined by the Abrahamson coherence function for soil sites (Abrahamson, 2007), also including an apparent horizontal wave velocity of 4500 fps in X-longitudinal direction to simulate the wave passage effects.

SASSI MODELING

The FE model mesh of the pile foundation part of the overall SSI model is shown in Figures 5 and 6. A total of about 200,000 nodes are included in this pile foundation model. The piles were modelled using linear-behaviour solid type elements that create a hexagonal cross-section approximating the circular shape of piles. In the pile axis soft beam elements are included, so that the pile forces and moments are easily extracted for comparisons of SSI results. The adjacent soil and soil between piles is modelled by solid elements considered with either linear or nonlinear hysteretic behaviour. The FE mesh is sufficiently refined to provide reasonably accurate stresses and strains in the soil elements that is important for including the nonlinear hysteretic soil behaviour.

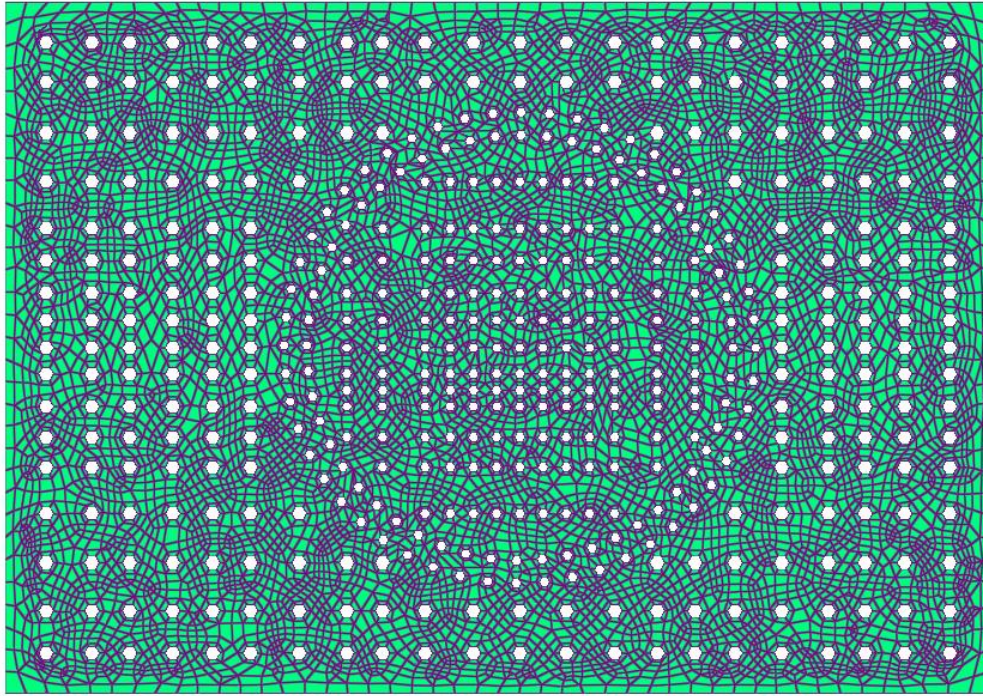


Figure 5. Pile Foundation Mesh at Each Embedment Soil Layer Level (about 12,500 nodes)

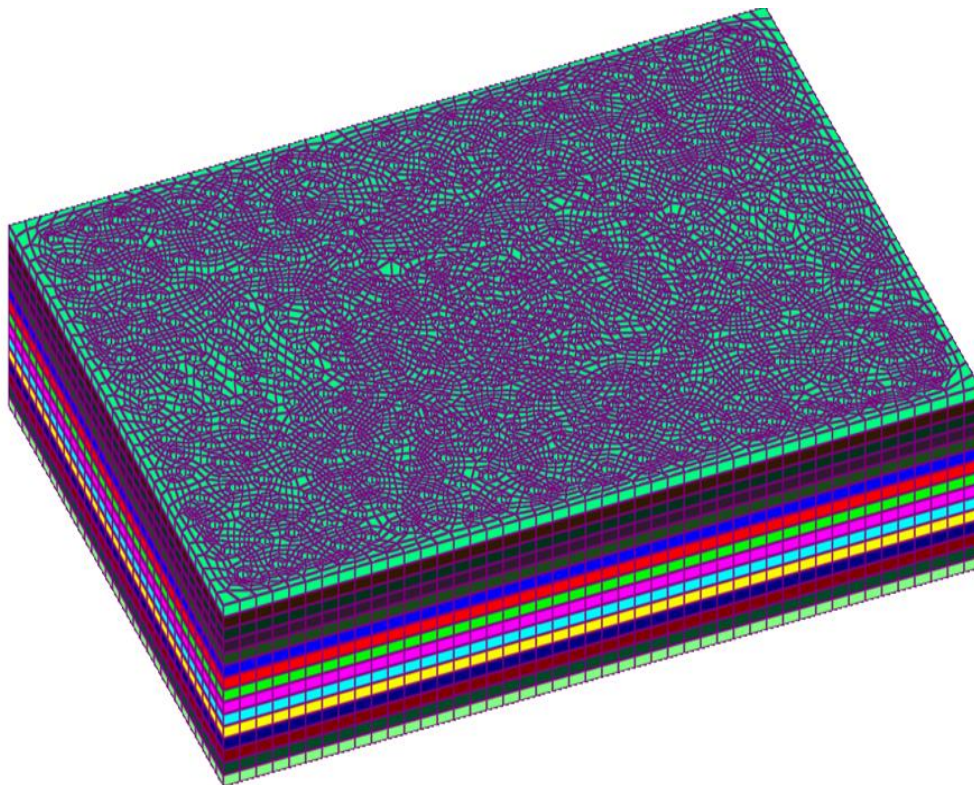


Figure 6. Pile Foundation Mesh Including All Embedment Soil Layer Levels (about 200,000 nodes)

The RB complex building basemat is assumed with no embedment sitting only on the concrete piles. It was assumed that the basemat was not transmitting directly any load pressure to the soil. The seismic basemat forces and moments are transmitted to the concrete piles only. This SSI modelling avoids on purpose including the potential basemat contribution to the overall pile foundation impedances.

One important SSI modelling remark associated to the application of the SASSI methodology is that the FE mesh of the soil is refined and irregular between piles, but it is coarser and regular at the external mesh boundaries were connected to the far-field soil layers and the excavated soil mesh. Because of this SSI modelling, the excavated soil model has a perfect regular mesh, that is important for capturing accurately the kinematic SSI or wave scattering effects which are significant for the deeply embedded pile foundation. At the same time this SSI modelling provides a high numerical efficiency. The entire SSI model of about a size of about 250,000 nodes was run on a 256 GB RAM PC workstation operating under the MS Window 10 system in less than 20 hours for 100 SSI frequencies (using the most recent ACS SASSI V4 software).

The SASSI modelling based on having a regular mesh for the excavated soil FE model as shown in Figures 5 and 6, is highly recommended by the USNRC BNL consultants (Nie, Braveman and Costantino, 2013).

COMPARATIVE SSI ANALYSIS RESULTS

In this section comparative SSI responses obtained are presented. Firstly, the comparative SSI results are presented between the cases “Without Piles” and “With Piles” for the Case A with the floating piles in a deep soil deposit, and the Case B with the peak-bearing piles penetrating through a 60 ft soft soil layer above a rock formation that provides a stiff support for the pile foundation.

Firstly, we compare the SSI analysis results assuming a linear soil behaviour in the vicinity of the piles.

Figures 7 and 8 show the SSI relative displacement histories at the basemat corner of the nuclear RB complex in the Y transverse horizontal and Z vertical directions with respect to the free-field control motion. Figure 7 compares “Without piles” and “With piles” results for the Case A of the floating piles in a deep soil profile, while Figure 8 compares results for the Case B of the peak-bearing piles in the rock formation.

The comparative SSI displacement results indicate the relative weak influence of the piles in the basemat horizontal response for both Cases A and B. However, this influence is almost negligible for the floating piles, but non-negligible for the peak-bearing piles. As expected, for the vertical direction, the effect of piles is small for the floating piles, and large for the peak-bearing piles. For the latter, the vertical displacements are reduced by the effect of the peak-bearing piles by an order of magnitude.

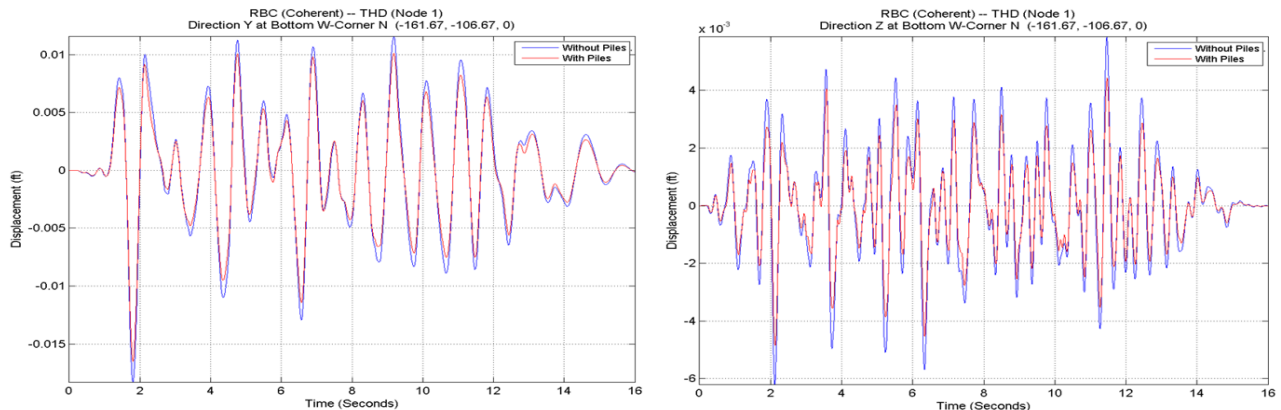


Figure 7. Case A Basemat SSI Relative Displacement Response in Y-horizontal (left) and Z-vertical (right) directions for “With Piles” and “Without Piles”

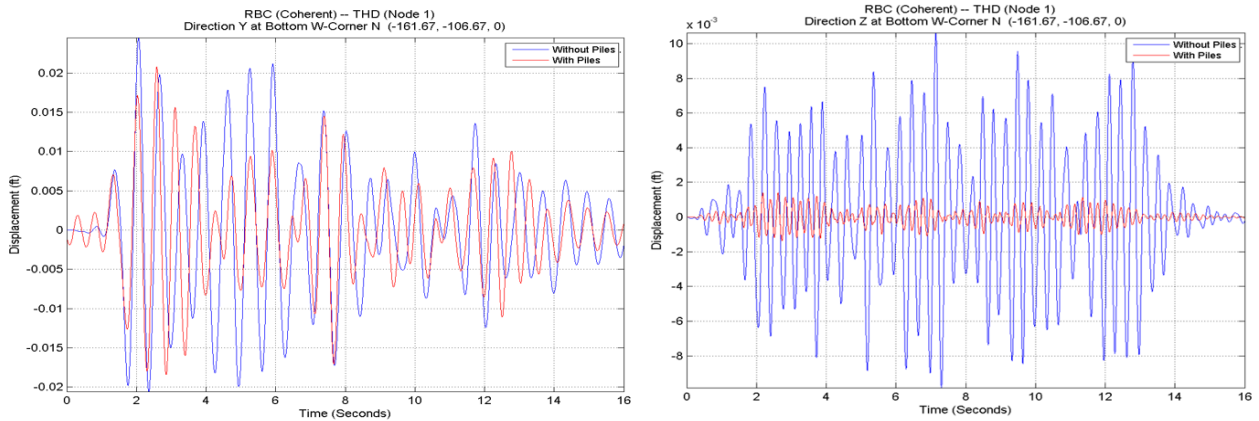


Figure 8. Case B Basemat SSI Relative Displacement Response in Y-horizontal (left) and Z-vertical (right) directions for “With Piles” and “Without Piles”

However, it should be noted that if 30 degree angle inclined S-P waves are considered instead of vertically propagating S-P waves, then the effectiveness of the piles for reducing the vertical displacements at the basemat corner is poorer, as shown in Figure 9. Inclined incident waves amplify both the horizontal and vertical relative displacement motions with respect to the free-field reference motion.

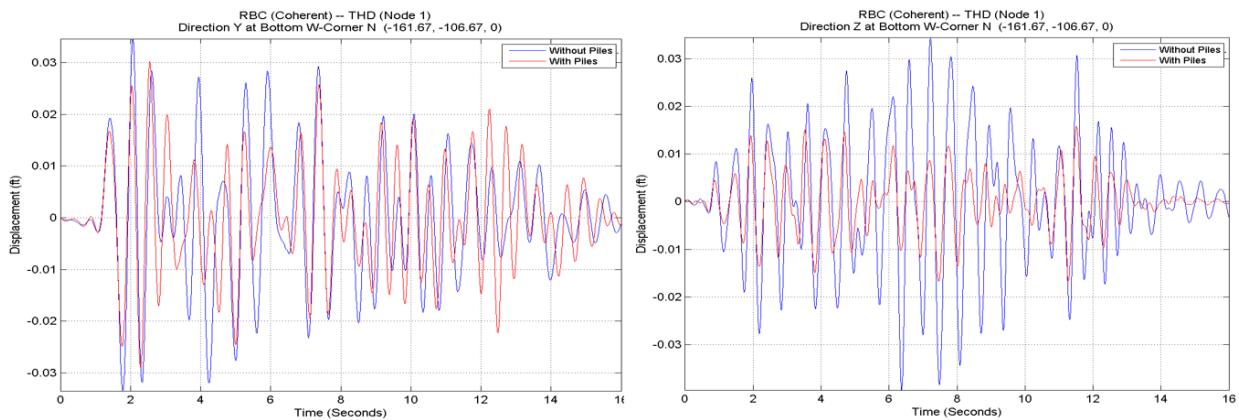


Figure 9. Case B Basemat SSI Relative Displacement Response in Y-horizontal (left) and Z-vertical (right) directions for “With Piles” and “Without Piles” Under 30 Degree Inclined S-P Waves

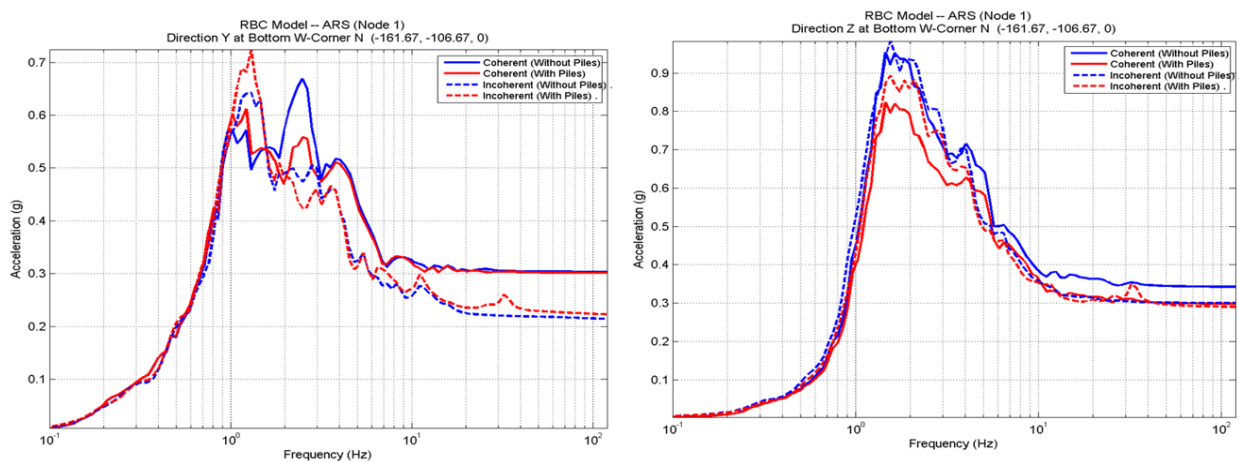


Figure 10 Case A Coherent and Incoherent ISRS in Y and Z directions for “With Piles” and “Without Piles”

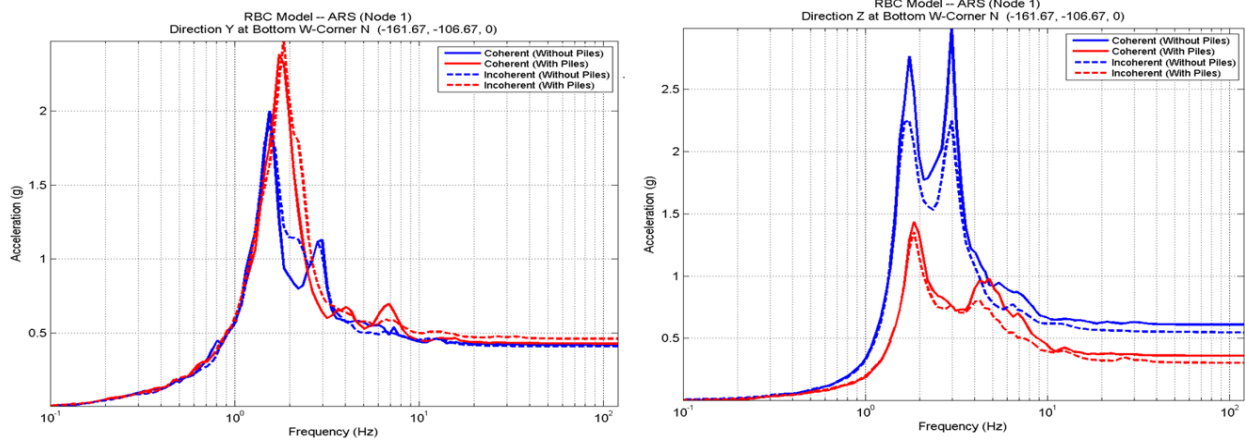


Figure 11 Case B Coherent and Incoherent ISRS in Y and Z directions for “With Piles” and “Without Piles”

Figures 10 and 11 show comparative ISRS computed at the basemat level for the Y and Z directions for the two cases of floating-piles and peak-bearing piles. The plotted ISRS results include both the coherent and the incoherent ISRS for “With Piles” and “Without Piles”. The ISRS differences reflect that same trends noticed for the SSI relative displacements. The effects of piles are minor for the floating-piles (Case A) and significant for the peak-bearing piles (Case B). It should be noted that the peak-bearing piles (Case B) amplify by about 20% the horizontal ISRS peak near 1.9 Hz which corresponds to the largest SSI mode of the system in the horizontal direction. This ISRS amplification is a result of the decrease of the SSI effects due to the reduction of the SSI rocking motion at the basemat level due to the significant vertical stiffness introduced by the peak-bearing piles. The largest ISRS peak in the vertical direction @ 3.0 Hz is largely reduced by the peak-bearing piles. The effects of the motion incoherency on ISRS appear to be mild, being only significant in the vertical direction for the peak-bearing piles with up to 30% reduction of ISRS peaks. For the floating piles, the minor increase of the ISRS peak around 1.5 Hz in horizontal direction at basemat corner is due to the torsion produced by incoherency.

The ISRS result trends shown in Figures 10 and 11 should be quite general for the nuclear complexes founded on floating piles or peak-bearing piles.

Figures 12 and 13 show the effects of the motion incoherency on the pile axial forces and bending moments for floating piles and peak-bearing piles. The selected pile location is at the corner of the pile foundation as indicated in Figure 2 (see the marked low-right corner pile, in Group 57, Pile 4).

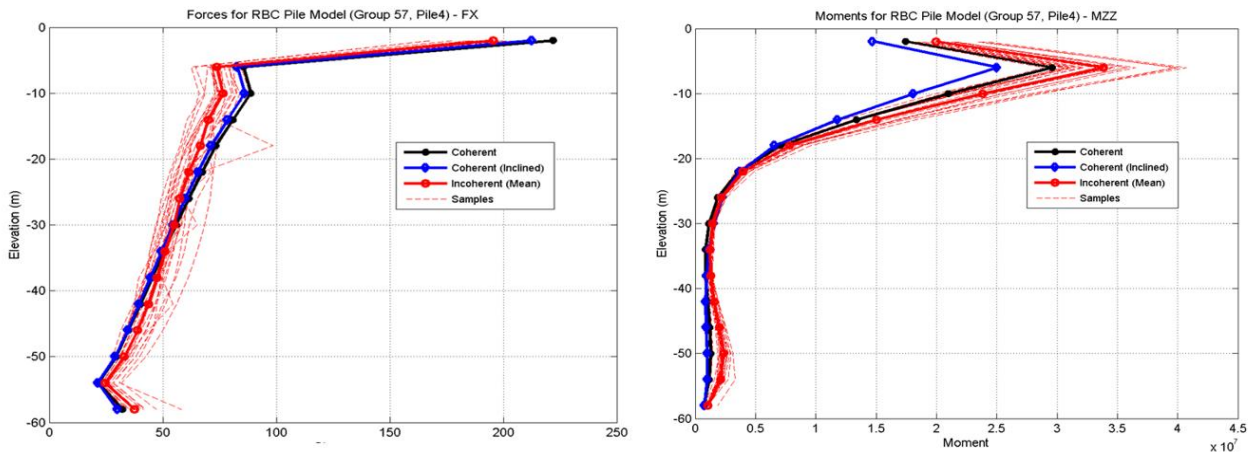


Figure 12 Case A Coherent vs. Incoherent Pile Maximum Axial Forces (left) and Bending Moments (right)

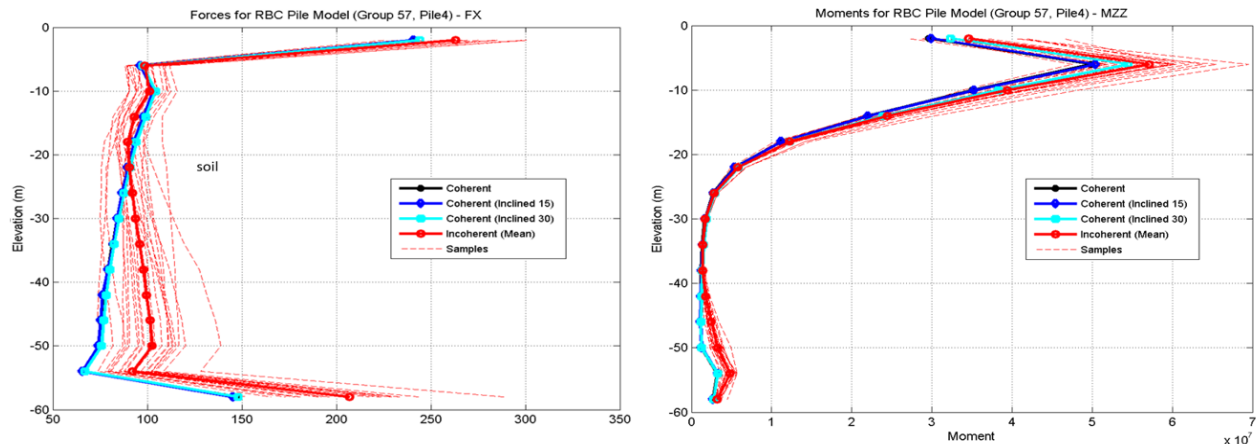


Figure 13 Case B Coherent vs. Incoherent Pile Maximum Axial Forces (left) and Bending Moments (right)

The coherent pile force/moment diagrams with depth are plotted with black line, while the incoherent pile diagrams are plotted with red lines (thick line for mean value and thin lines for the 20 samples).

Figures 12 and 13 also includes results obtained for the inclined S-P incident waves with 15 and 30 degrees angles with the vertical direction. The wave inclination effects are minor for the pile forces and moments.

From Figures 12 and 13, it should be noted that the motion incoherency increases the pile maximum bending moments by about 15% at lower depth under basemat for both the floating piles and the peak-bearing piles, and also increases the pile maximum axial forces by up to 30% for the peak-bearing piles at large depths close to the rock formation. For the floating piles, the increase of the pile axial forces due to incoherency is minor. These remarks are valid for the foundation corner piles. For the foundation center piles, the incoherency effects trends are favourable.

NONLINEAR SOIL HYSTERETIC BEHAVIOR IN VICINITY OF PILES

In this section, the effects of the local hysteretic soil material behaviour in the vicinity of piles is investigated. Only Case B with the peak-bearing piles is considered. The local nonlinear soil behaviour was modelled using an iterative equivalent-linearization procedure, in principle similar with the procedure included the SHAKE code for the 1D layered soil models (Idriss and Sun, 1992).

However, the local nonlinear soil behaviour effects in the 3D soil space of the FE model, the shear modulus and damping soil material curves are considered as functions of the local octahedral shear strain computed in each soil solid element. After each linearized SSI analysis iteration, to avoid making linear superpositions that will be incorrect for nonlinear analysis, the octahedral shear strains computed for each input direction, X, Y and Z are combined before considering the hysteretic soil behaviour for each soil element. This iterative equivalent-linearization SSI analysis is performed automatically in ACS SASSI (Ghiocel, 2019).

Various comparative results are shown in Figures 14 through 20. Figures 14 and 15 show the relative displacements of the basemat and high-elevation locations within the nuclear RB complex with respect to the free-field motion. The nonlinear hysteretic soil behaviour amplifies the horizontal displacement response and produces no effect on the vertical displacement response.

The effects of local nonlinear soil behaviour in the vicinity of piles are quite large and beneficial on the ISRS, as shown in Figures 16, 17 and 18 for three locations at different elevations within the RB complex.

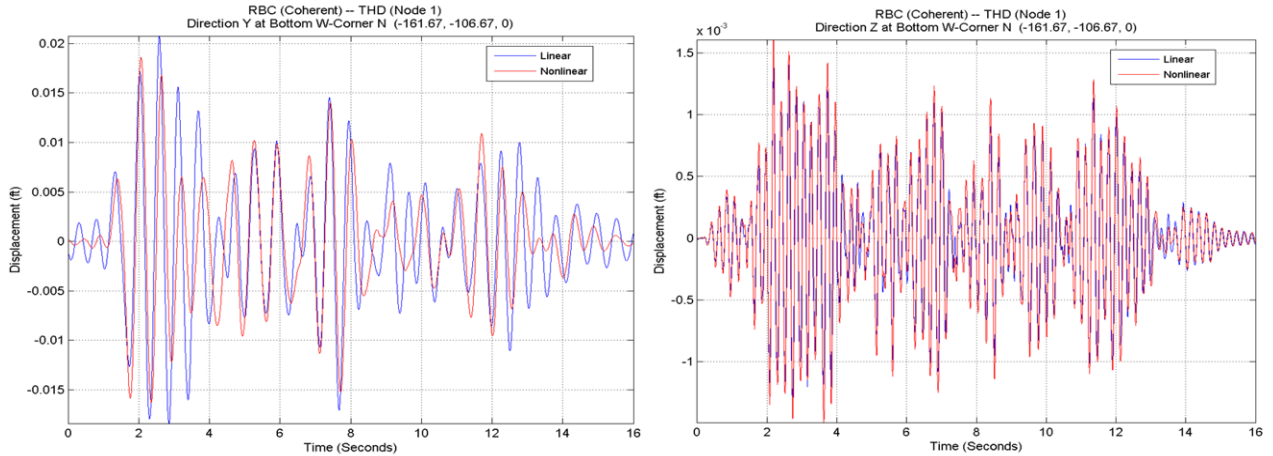


Figure 14 Linear vs. Nonlinear Relative Displacement at the Basemat Level for Y and Z directions.

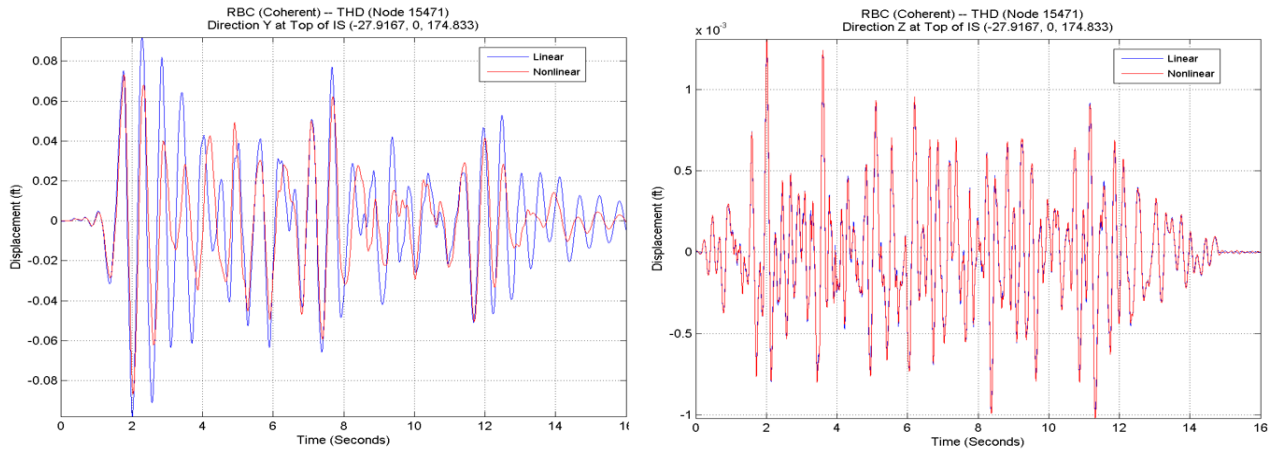


Figure 15 Linear vs. Nonlinear SSI Relative Displacements at High-Elevation Level for Y and Z directions

From Figures 16, 17 and 18, it should be noted that the SSI dominant ISRS spectral peak @ 1.9 Hz is largely reduced due to the nonlinear hysteretic soil behaviour for both horizontal and vertical directions. This is a result of the soil material damping increase near piles from 3% in the free-field to 8-15% between the piles.

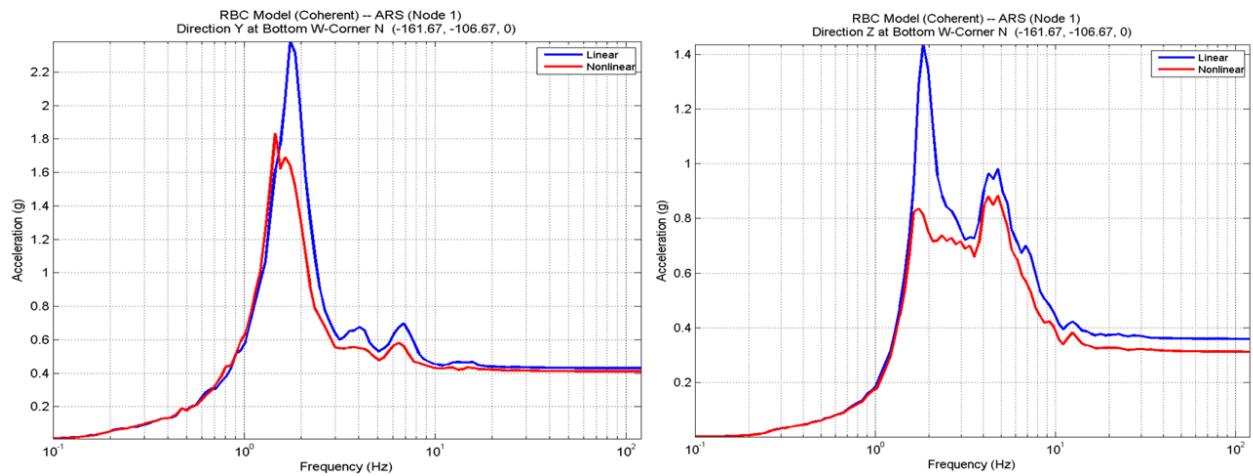


Figure 16 ISRS for Linear vs. Nonlinear Soil Behaviour at the Basemat Level for Y and Z directions.

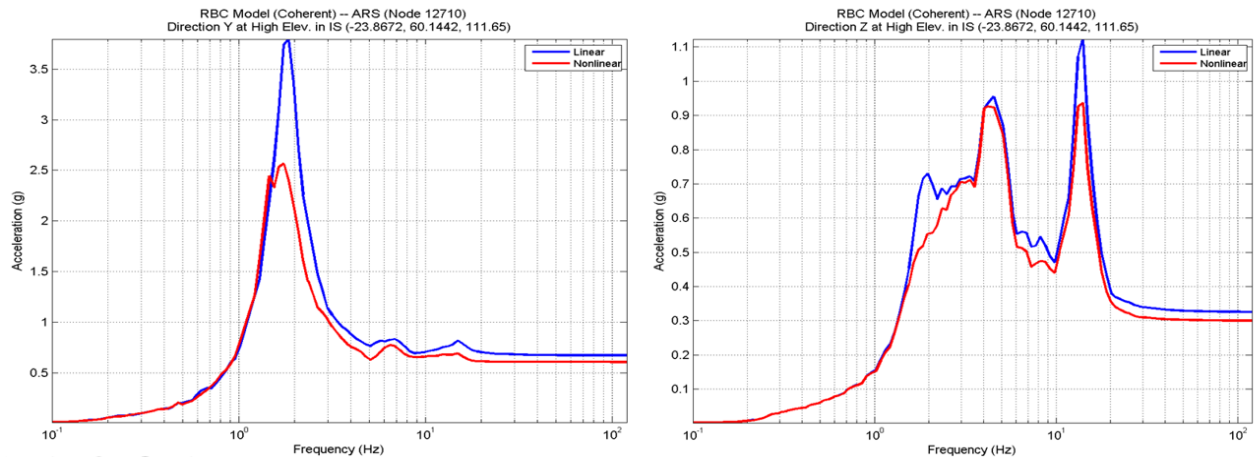


Figure 17 ISRS for Linear vs. Nonlinear Soil Behaviour at High Elevation 112 ft for Y and Z directions

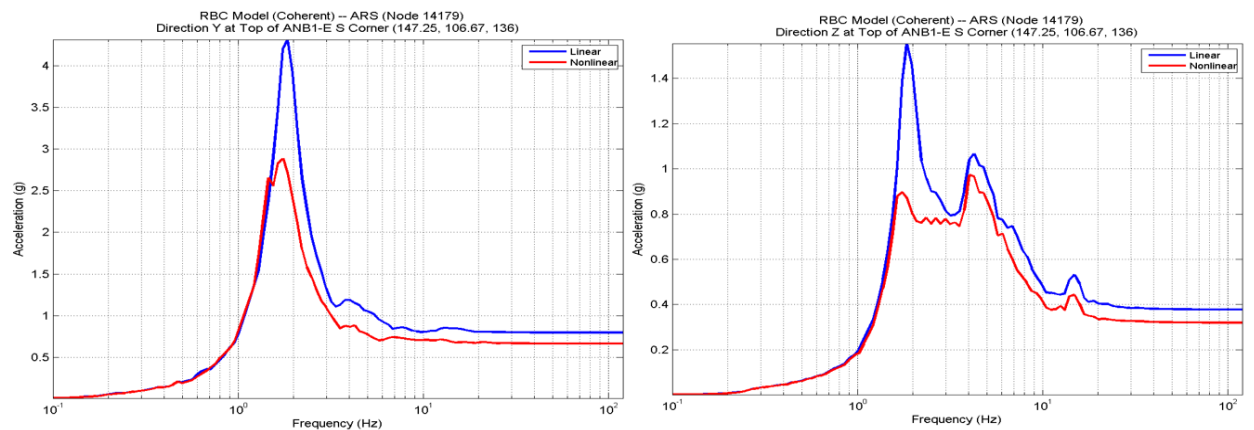


Figure 18 ISRS for Linear vs. Nonlinear Soil Behaviour at Top Elevation 136 ft for Y and Z directions

It is also remarked that the nonlinear soil behaviour produces a shift of the SSI dominant ISRS spectral peak from @ 1.9 Hz to @ 1.6 Hz. This ISRS spectral peak reduction is visible in all three figures.

Figures 19 and 20 show the effects of the nonlinear soil behaviour on the pile axial forces and bending moments. Two pile locations are selected. Figure 19 shows results for a pile located in the center of the pile foundation, while Figure 20 shows results for a pile close to the transverse edge as described in Figure 2.

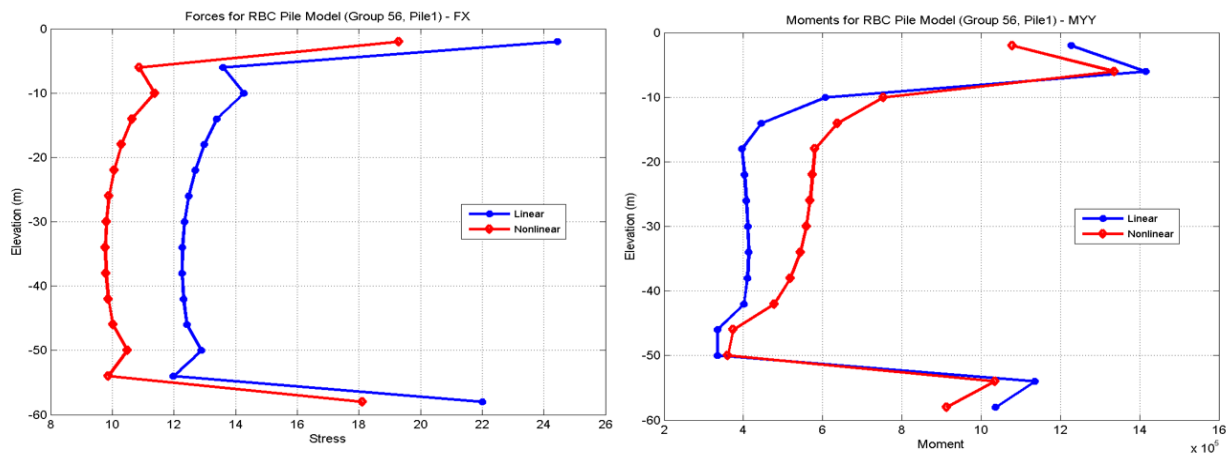


Figure 19 Center Pile Maximum Axial Forces and Bending Moments for Linear vs. Nonlinear Soil

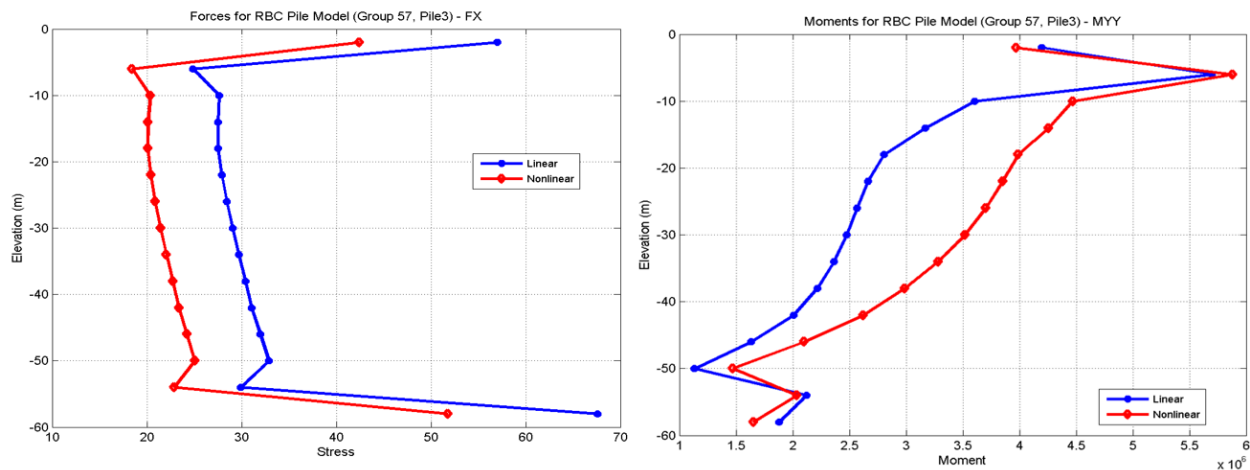


Figure 20 Close to Edge Pile Maximum Axial Forces and Bending Moments for Linear vs. Nonlinear Soil

From the Figures 19 and 20, it should be noted that the soil nonlinear behaviour reduces the seismic axial forces in piles, most likely as a result of reducing the building accelerations and the vertical seismic loads on piles. Due to the nonlinear soil behaviour, the pile bending moments increase in the middle depth range, and slightly decrease at the top and bottom extremes of the piles.

CONCLUDING REMARKS

The paper describes an accurate and efficient SSI modelling for the pile foundation. Computed results show that the pile influence on various SSI responses is weak for the floating piles, and much more significant for the peak-bearing piles.

The motion incoherency effects are less significant since the SSI system is a low frequency oscillating system with SSI dominant frequency in the 1-2 Hz range. However, the motion incoherency can increase the pile axial forces and bending moments.

The nonlinear hysteretic soil behaviour in the vicinity of the piles reduces significantly the RB complex ISRS spectral peaks due to the large increase in the local soil material damping in the vicinity of piles.

REFERENCES

- Abrahamson, N. (2007). "Effects of Spatial Incoherence on Seismic Ground Motions", Electric Power Research Institute Report No. TR-1015110, Palo Alto, CA and US Department of Energy, Germantown, MD, December 20
- Ghiocel Predictive Technologies, Inc. (2019). "ACS SASSI - An Advanced Computational Software for 3D Dynamic Analyses Including SSI Effects", *ACS SASSI Version 4 User Manuals, Revision 0*, Rochester, New York
- Nie, J., Braverman, J., and Costantino, M. (2013). "Seismic Soil-Structure Interaction Analyses of A Deeply Embedded Model Reactor – SASSI Analyses", *U.S. Department of Energy, Brookhaven National Laboratory, BNL 102434-2013*, New York
- Idriss I.M, Sun J.I (1992) "SHAKE 91: A Computer Program for Conducting Equivalent Linear Seismic Response Analyses of Horizontally Layered Soil Deposits", *Technical Report at Department of Civil Engineering, University of California, Davis*